



Iron isotope evidence for very rapid accretion and differentiation of the proto-Earth

Schiller, Martin; Bizzarro, Martin; Siebert, Julien

Published in:
Science Advances

DOI:
[10.1126/sciadv.aay7604](https://doi.org/10.1126/sciadv.aay7604)

Publication date:
2020

Document version
Publisher's PDF, also known as Version of record

Document license:
[CC BY-NC](#)

Citation for published version (APA):
Schiller, M., Bizzarro, M., & Siebert, J. (2020). Iron isotope evidence for very rapid accretion and differentiation of the proto-Earth. *Science Advances*, 6(7), [eaay7604]. <https://doi.org/10.1126/sciadv.aay7604>

PLANETARY SCIENCE

Iron isotope evidence for very rapid accretion and differentiation of the proto-Earth

Martin Schiller^{1*}, Martin Bizzarro^{1,2}, Julien Siebert^{2,3}

Nucleosynthetic isotope variability among solar system objects provides insights into the accretion history of terrestrial planets. We report on the nucleosynthetic Fe isotope composition ($\mu^{54}\text{Fe}$) of various meteorites and show that the only material matching the terrestrial composition is CI (Ivuna-type) carbonaceous chondrites, which represent the bulk solar system composition. All other meteorites, including carbonaceous, ordinary, and enstatite chondrites, record excesses in $\mu^{54}\text{Fe}$. This observation is inconsistent with protracted growth of Earth by stochastic collisional accretion, which predicts a $\mu^{54}\text{Fe}$ value reflecting a mixture of the various meteorite parent bodies. Instead, our results suggest a rapid accretion and differentiation of Earth during the ~5-million year disk lifetime, when the volatile-rich CI-like material is accreted to the proto-Sun via the inner disk.

INTRODUCTION

Terrestrial planet formation is thought to occur in stages, where first-generation bodies of a few hundred kilometer radii form rapidly by streaming instabilities, followed by growth dominated by gas drag-assisted accretion of millimeter-sized particles onto these bodies (1) to form Mars-sized planetary embryos during the protoplanetary disk stage. In the inner solar system, these embryos are inferred to have formed from thermally processed and, hence, dry and reduced solids. After dissipation of the gas, the terrestrial planets are assembled over several tens of millions of years via large collisions between embryos (2), many of which will have differentiated into metal cores and silicate mantles. In these models, water and other volatile elements are inferred to have been delivered to Earth and oxidized its mantle during the last phase of accretion after core formation, possibly by volatile-rich, outer solar system bodies scattered inward by the outward migration of Jupiter (3–5). However, a recent study of the isotope composition of the siderophile element ruthenium in solar system objects, including Earth and the parent bodies of chondrite meteorites, suggests that Earth's volatile element budget may have been acquired much earlier (6), perhaps during its main accretion phase. Moreover, new planet formation models based on the rapid accretion of pebbles onto asteroidal seeds suggest that Earth's main accretion phase may have been completed within the ~5-million year lifetime of the protoplanetary disk (1). Elucidating the accretion history of Earth, including the timing of addition of volatile elements, is critical for a full understanding of the timescales of terrestrial planet formation.

Mass-independent isotope variability of nucleosynthetic origin among early solar system objects can be used to track the source and nature of the material precursor to the terrestrial planets. In particular, iron is a redox-sensitive, siderophile major element whose partitioning between mantle and core is a proxy of the overall oxidation state of a planet. Iron readily oxidizes in the presence of water, substantially lowering its partitioning into the metal core (7, 8). Therefore, if Earth became more oxidized during accretion and core formation, the mass-independent Fe isotope composition of Earth's man-

tle is predicted to be dominated by that of the late accreting material. The existence of nucleosynthetic Fe isotope variability in solar system objects can thus provide a powerful tool to fingerprint the source of the material responsible for the delivery of water to Earth and the subsequent oxidation of Earth's mantle.

RESULTS

CI chondrites are believed to best represent the bulk solar system composition for most elements and, hence, that of the Sun (9). Thus, CI chondrites best approximate the average composition of the molecular cloud material that collapsed to form the Sun and its planets. To evaluate the nucleosynthetic iron isotope variability in the solar system, we have subjected the Ivuna CI chondrite to a stepwise leaching procedure that provides a crude chemical separation of its various mineralogical components (10). This experiment reveals the existence of two main carriers of Fe nucleosynthetic variability, expressed as the $\mu^{54}\text{Fe}$ value (see Materials and Methods), each comprising about half the total iron budget in this meteorite (Fig. 1A and Table 1). Labile phases dissolved in the early dissolution steps (L2 to L7) exhibit elevated $\mu^{54}\text{Fe}$ values of around +46 parts per million (ppm) with respect to Earth's mantle, which we interpret as reflecting the average composition of phases isotopically homogenized during parent body processes. Later dissolution steps (L8 to L12) contain both negative and positive $\mu^{54}\text{Fe}$ values that range from –82 to +273 ppm in dissolution steps L8 and L11, respectively. This provides evidence for the presence of presolar carriers of nucleosynthetic Fe isotope heterogeneity. Hence, variable incorporation of these carriers in disk solids, including asteroidal and planetary bodies, could impart resolvable solar system-wide iron isotope heterogeneity.

To determine the $\mu^{54}\text{Fe}$ composition of the disk material that may have contributed to the growth of terrestrial planets, we measured the $\mu^{54}\text{Fe}$ value of various classes of chondrites and their main constituents, namely, individual chondrules, as well as that of meteorites originating from differentiated parent bodies (Fig. 1B and Table 2). Apart from CI chondrites, which have a $\mu^{54}\text{Fe}$ indistinguishable from Earth's mantle, all chondrites are characterized by resolvable excesses in $\mu^{54}\text{Fe}$ ranging from $+6.4 \pm 0.7$ ppm to $+28.8 \pm 4.4$ ppm relative to Earth's mantle. Similarly, samples of differentiated bodies represented by iron meteorites record $\mu^{54}\text{Fe}$ excesses, in agreement with an earlier report (11). The ordinary and CR2 chondrite chondrules

¹Centre for Star and Planet Formation, Globe Institute, University of Copenhagen, Øster Voldgade 5–7, DK-1350 Copenhagen, Denmark. ²Institut de Physique du Globe de Paris, Université Sorbonne Paris Cité, 75005 Paris, France. ³Institut Universitaire de France, Paris, France.

*Corresponding author. Email: schiller@ign.ku.dk

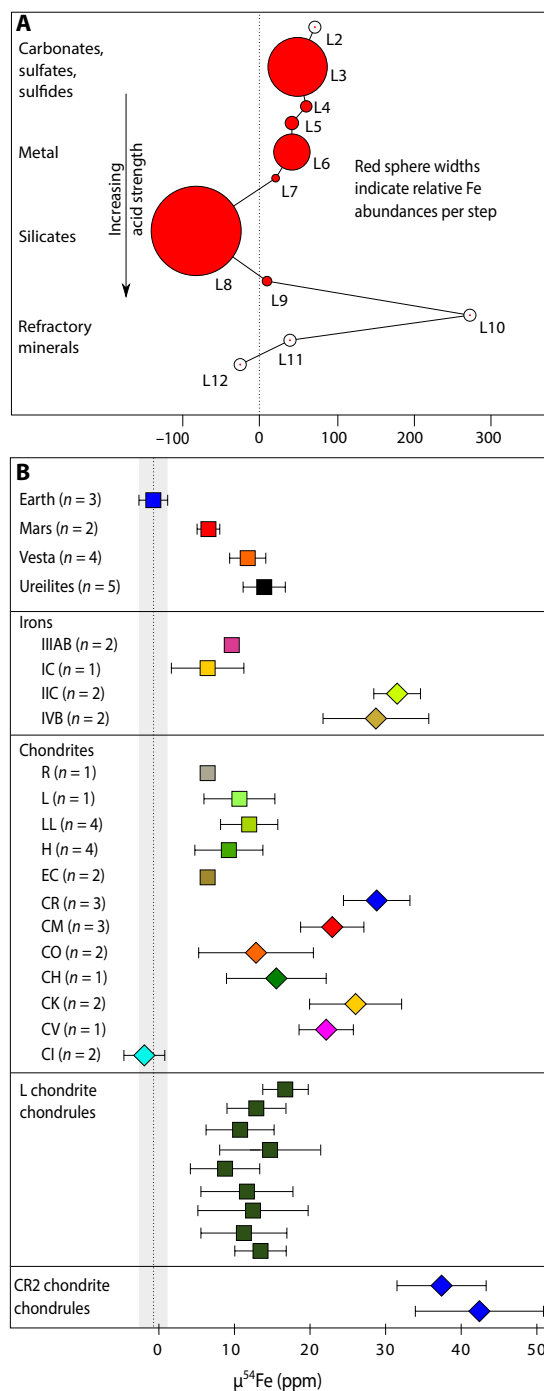


Fig. 1. $\mu^{54}\text{Fe}$ data of a stepwise dissolution experiment of the CI chondrite Ivuna and bulk silicate Earth, stony and iron meteorites, chondrites, and chondrules. (A) Plot of $\mu^{54}\text{Fe}$ values measured in steps of increasing acid strength (L2 to L12) of a dissolution experiment of ~ 3 g of the CI chondrite Ivuna (10). Width of spheres indicates the relative proportion of iron in dissolution steps. Uncertainties for individual measurements are typically smaller than the symbols and not shown (Table 1). (B) Average $\mu^{54}\text{Fe}$ values for each group of samples from distinct solar system reservoirs (Table 2), where n denotes the number individual samples measured. The uncertainties shown for individual data points reflect either two times the SE (2 SE) of the average of the mean of the analyses or the 2 SE of the sample analysis if the group only consists of one sample without replicate analyses. The vertical dotted line and shaded area represent the mean value for terrestrial standards (10 individual analyses) and the 2 SE of these data.

Table 1. Mass-independent $\mu^{54}\text{Fe}$ and mass-dependent $\delta^{56}\text{Fe}$ values for sequential dissolution steps of the CI chondrite Ivuna. The combined average iron isotope signature of the individual dissolution steps is consistent with the whole rock data. The number of repeat analyses of each dissolution steps is indicated by n .

Dissolution step	$\mu^{54}\text{Fe} \pm 2 \text{ SE}$ (ppm)	$\delta^{56}\text{Fe} \pm 2 \text{ SE}$ (‰)	%Fe _{total}	n
L2	71 ± 4.1	-0.95 ± 0.02	0.37	10
L3	49.1 ± 6.1	-0.41 ± 0.02	25.57	10
L4	59.4 ± 4.2	-0.58 ± 0.03	4.89	10
L5	43.3 ± 4.4	-0.20 ± 0.02	6.26	10
L6	42.1 ± 5.6	-0.06 ± 0.03	16.01	10
L7	21.0 ± 3.4	-0.33 ± 0.03	2.94	10
L8	-81.5 ± 3.2	0.54 ± 0.03	39.54	10
L9	9.3 ± 2.9	-0.16 ± 0.02	4.24	10
L10	39.6 ± 4.4	0.44 ± 0.05	0.10	10
L11	272.5 ± 7.6	0.24 ± 0.02	0.05	5
L12	-23 ± 14	0.52 ± 0.03	0.01	5
Average/sum	-5.9	0.04	100.00	

are also all variably enriched in ^{54}Fe comparable to their host meteorites, where the two CR2 chondrules exhibit the highest $\mu^{54}\text{Fe}$ values of the analyzed samples (Fig. 1). Collectively, our data establish that apart from CI chondrites, none of the meteorites analyzed here, including all main chondrite groups, match the terrestrial composition. A CI-like composition of Earth's mantle is not observed for other siderophile nucleosynthetic tracers such as Mo and Ru. However, these elements are much more siderophile than Fe and, as such, their compositions can be easily modified by late accretion events such as the Moon-forming impact and/or addition of the later veneer material. Unlike Fe, which records the dominant source of the material that accreted to Earth after the onset of core formation, Mo and Ru are understood to only track the last $\sim 10\%$ of the terrestrial accretion. Hence, the observation that the bulk of the Fe in the terrestrial mantle is indistinguishable from CI chondrites has far-reaching implications for understanding the accretion history of Earth.

DISCUSSION

Earth's main accretion phase is understood to have occurred via stochastic collisional accretion of embryos and planetesimals over several tens of millions of years (2, 12). In this model, oxidation of Earth's mantle occurs toward the end of the accretion by increased addition of oxidized, outer solar system impactors, once the initially more reduced proto-Earth has differentiated and reached approximately 80% of its current mass (3–5, 13–15). Thus, if Earth's mantle iron content was derived from the accretion of oxidized outer solar system bodies, the $\mu^{54}\text{Fe}$ composition of the terrestrial mantle should be dominated by an average carbonaceous chondrite-like composition. However, the only chondrite group that matches the terrestrial composition is CI chondrites. Apart from the metal-rich carbonaceous chondrites, which may have accreted beyond the orbits of the gas giants, most carbonaceous chondrites are believed to have formed near the snow line beyond Jupiter or, alternatively, in the outer asteroid

Table 2. Iron isotope compositions of bulk meteorites and chondrules.

Summary of the mean mass fractionation–corrected ($\mu^{54}\text{Fe}$) and mass-dependent ($\delta^{56}\text{Fe}$) iron isotope composition of cores and mantles of asteroidal and planetary bodies, chondrites, and individual chondrules. The number of individual analyses including distinct samples or repeat analyses of the same sample is indicated by n . Results for individual analyses can be found in table S1.

	$\mu^{54}\text{Fe} \pm 2 \text{ SE}$ (ppm)	$\delta^{56}\text{Fe} \pm 2 \text{ SE}$ (‰)	n
Planetary mantles			
Earth	-0.8 ± 1.9	0.04 ± 0.04	10
Mars	6.5 ± 1.5	0.00 ± 0.04	4
Vesta	11.7 ± 2.4	0.05 ± 0.06	5
Ureilites	13.9 ± 2.8	0.02 ± 0.02	8
Irons			
IC	6.4 ± 4.8	0.07 ± 0.01	1
IIIAB	9.6 ± 0.4	0.00 ± 0.05	2
IVB	28.7 ± 7.0	0.03 ± 0.01	2
IIC	31.5 ± 3.1	0.00 ± 0.03	2
Chondrites			
OC	10.5 ± 2.6	-0.03 ± 0.01	9
R	6.4 ± 0.8	-0.02 ± 0.01	1
EC	6.4 ± 0.7	0.06 ± 0.07	4
CR	28.8 ± 4.4	0.05 ± 0.07	3
CM	22.9 ± 4.2	0.00 ± 0.01	3
CO	12.8 ± 7.6	-0.01 ± 0.00	2
CH	15.5 ± 6.6	-0.04 ± 0.01	1
CK	26.0 ± 6.1	-0.01 ± 0.05	2
CV	22.1 ± 3.6	-0.06 ± 0.01	1
CI	-2.0 ± 2.7	0.06 ± 0.03	9
Ordinary chondrite chondrules			
2-C1	16.7 ± 3.0	0.70 ± 0.04	
5-C2	12.9 ± 3.9	1.39 ± 0.02	
5-C10	10.7 ± 4.5	1.38 ± 0.03	
D-C3	14.7 ± 6.7	0.12 ± 0.03	
5-C4	8.7 ± 4.6	-0.23 ± 0.03	
3-C5	11.6 ± 6.1	0.00 ± 0.05	
11-C1	12.4 ± 7.3	-0.19 ± 0.01	
11-C2	11.2 ± 5.7	0.05 ± 0.01	
3-C2	13.4 ± 3.4	0.04 ± 0.08	
CR2 chondrite chondrules			
1-C2	37.4 ± 5.9	0.04 ± 0.01	
2-C4	42.4 ± 8.5	0.04 ± 0.02	

belt (16). Thus, it is highly improbable that scattering of outer solar system bodies by the inward migration of Jupiter would result in the selective delivery of only one type of the outer solar system material to Earth's feeding zone, namely, CI chondrites. Alternatively, the bulk of the iron in Earth's mantle could originate from the impact of a single body with a CI-like composition such as, for example, the

Moon-forming impact. However, using the most conservative estimates for the $\mu^{54}\text{Fe}$ composition and iron concentration of the proto-Earth as well as that of the impactor (see Materials and Methods), mass balance arguments require at least a body with a mass of approximately 15 to 20% of that of the proto-Earth, which corresponds to a planetary embryo. As planetary embryos are understood to grow by the combined effect of pebble and planetesimal accretion (1), it is unlikely that this process will result in a purely CI-like $\mu^{54}\text{Fe}$ composition given the extent of nucleosynthetic diversity that exists among outer solar system bodies (Fig. 1). Thus, the CI chondrite composition of Earth's mantle is inconsistent with the idea that Earth's main accretion phase before the Moon-forming impact was dominated by stochastic collisional accretion of planetesimals and planetary embryos. Moreover, a CI-like Moon-forming impactor as the origin of the CI-like composition of Earth's mantle is also inconsistent with the titanium and calcium isotopic similarity of Earth and Moon (17, 18). Current giant impact models cannot achieve the very high degree of isotopic equilibration between the two bodies required in the case of a carbonaceous impactor (19). Thus, we conclude that the CI-like composition of Earth's mantle cannot result from a carbonaceous, outer solar system Moon-forming impactor.

The only epoch in the history of the solar system when the CI-like material is readily available within the terrestrial planet-forming region is during the lifetime of the protoplanetary disk. This period represents the time when the in-falling envelope material of CI composition is channeled through the disk to fuel the growth of the proto-Sun and is estimated to have lasted approximately 4.8 ± 0.3 million years (Ma) (20). It has been suggested that the nucleosynthetic variability of the lithophile element calcium ($\mu^{48}\text{Ca}$) observed among inner solar system bodies, including Mars and proto-Earth, reflects the progressive admixing of the in-falling CI-like material during the disk's lifetime (18). In this framework, the dry and reduced material is rapidly locked into sizeable asteroidal bodies and planetary embryos, which continue to grow by the accretion of pebbles with a CI-like composition. Thus, the $\mu^{48}\text{Ca}$ isotope composition of terrestrial planets reflects mixtures of two reservoirs, namely, the thermally processed (and reduced) inner disk material and the pristine, volatile-rich CI-like envelope material. In this model, ureilite meteorites, which are characterized by the lowest $\mu^{48}\text{Ca}$ values among bulk solar system materials, are our best proxy for the isotope composition of the reduced, thermally processed inner disk material before admixing of the volatile-rich CI material (18). This mixing relationship between the CI-like material and ureilites is broadly consistent with that deduced from other lithophile nucleosynthetic tracers (see the Supplementary Materials). In Fig. 2, we show that the $\mu^{48}\text{Ca}$ and $\mu^{54}\text{Fe}$ systematics of the inner solar system material that avoided core formation like ordinary and enstatite chondrites as well as individual ordinary chondrite chondrules are coupled and form a simple mixing line. This observation is consistent with the idea that their compositions primarily result from binary mixing. However, given the distinct geochemical behavior of Fe and Ca, core formation occurring early in the accretion history of a planetary body, especially during accretion under reducing conditions, will result in decoupling of the $\mu^{48}\text{Ca}$ - $\mu^{54}\text{Fe}$ systematics. Notably, the mantle $\mu^{48}\text{Ca}$ - $\mu^{54}\text{Fe}$ systematics of Vesta (the parent body of howardite-eucrite-diogenite meteorites) and Mars are not decoupled, considering the level of precision of our data. This is consistent with the accretion of Mars under oxidizing conditions, where iron is more lithophile, and the very early and fast accretion of Vesta such that little accretion occurred

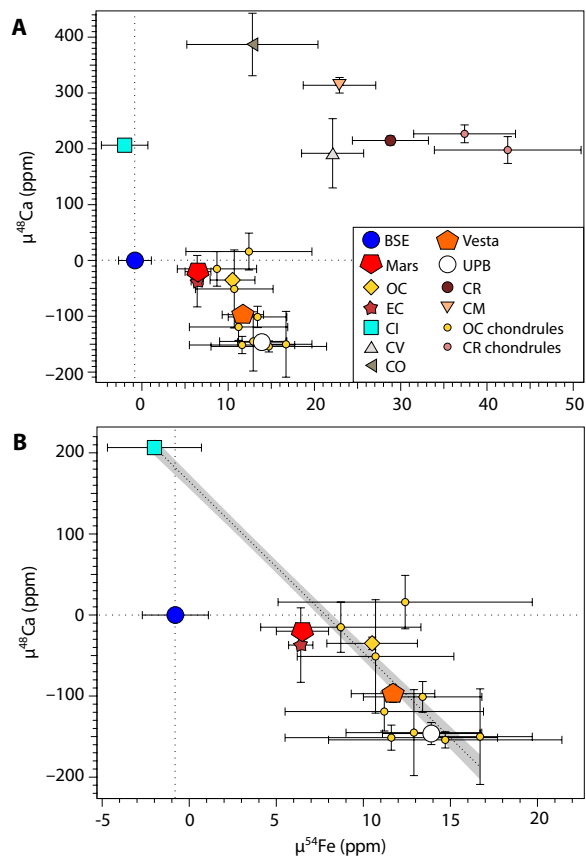


Fig. 2. Plots of $\mu^{54}\text{Fe}$ versus $\mu^{48}\text{Ca}$ values of bulk and bulk silicate solar system objects. (A) $\mu^{48}\text{Ca}$ (10, 18, 38) versus $\mu^{54}\text{Fe}$ plot of carbonaceous (outer solar system) and noncarbonaceous (inner solar system) objects. (B) $\mu^{48}\text{Ca}$ versus $\mu^{54}\text{Fe}$ plot of inner solar system objects plus CI chondrites. The linear regression includes ordinary chondrite chondrites, the ureilite parent body (UPB), as well as ordinary, enstatite, and CI chondrites, where the shaded area represents the 95% confidence interval. Uncertainties for both $\mu^{54}\text{Fe}$ and $\mu^{48}\text{Ca}$ are the 2 SE of the mean apart from $\mu^{48}\text{Ca}$ values for CO and CV, where they are the 95% confidence interval.

after segregation of its core (Figs. 2 and 3). In contrast to $\mu^{48}\text{Ca}$, the $\mu^{54}\text{Fe}$ value of the terrestrial mantle is dominated by a CI composition. This observation points to substantial decoupling of the terrestrial $\mu^{48}\text{Ca}$ - $\mu^{54}\text{Fe}$ systematics and requires that the bulk of the iron in the proto-Earth was already partitioned into a metallic core before the admixing of the CI-like material.

Earth's mantle CI-like iron isotope composition also constrains the timing of the Earth's oxidation, as it implies that the iron budget of the mantle was established during the lifetime of the protoplanetary disk when pebble accretion could operate. The proto-Earth accreting under more oxidizing conditions than today (21–23), however, is not compatible with the CI-like iron isotope composition of Earth's mantle (Fig. 3). Although the $\mu^{48}\text{Ca}$ - $\mu^{54}\text{Fe}$ systematics do not rule a constant oxidation state throughout Earth's accretion, this would require early and instantaneous core formation, followed by the accretion of only the CI-like material (Fig. 3), making this scenario unlikely. An initially more reduced proto-Earth relaxes these constraints and only requires that Earth oxidized (i.e., acquired most of its mantle iron budget) by the accretion of CI-like dust. Water is the key ingredient for oxidation (7, 8), and as such, our results

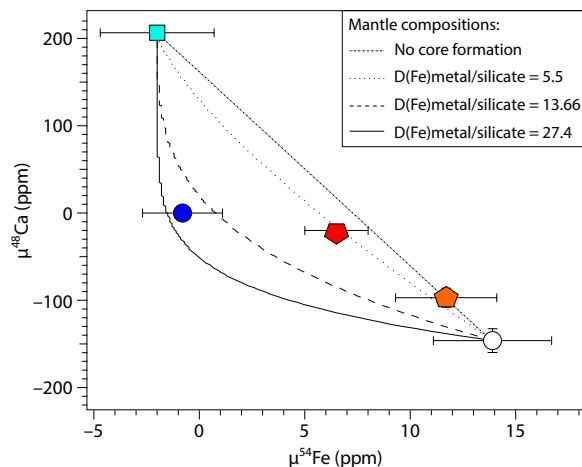


Fig. 3. Plot of $\mu^{48}\text{Ca}$ versus $\mu^{54}\text{Fe}$ of silicate mantles of inner solar system asteroids and planets and CI chondrites with possible accretion trajectories. $\mu^{54}\text{Fe}$ values are shown versus $\mu^{48}\text{Ca}$ data (10, 18) for the mantles of Earth, Mars, Vesta, and the UPB, where an increase in $\mu^{48}\text{Ca}$ represents addition of CI-like solids to the planetary objects (18). Symbols and uncertainties are the same as in Fig. 2. Shown trajectories for the evolution of the $\mu^{48}\text{Ca}$ - $\mu^{54}\text{Fe}$ mantle composition of a growing planetary body in the inner solar system assume either no core formation or core formation on a planetary body with initially UPB-like composition and subsequent addition of CI-like dust with distinct degrees of iron partitioning between core and mantle [$D(\text{Fe})_{\text{metal/silicate}}$] that are held constant throughout accretion. We show the isotopic evolution of a putative mantle composition in $\mu^{48}\text{Ca}$ - $\mu^{54}\text{Fe}$ space for three $D(\text{Fe})_{\text{metal/silicate}}$ values: one reflecting iron partitioning similar to that recorded by Earth today [$D(\text{Fe})_{\text{metal/silicate}} = 13.66$], as well as for accretion under more reducing [$D(\text{Fe})_{\text{metal/silicate}} = 27.4$] or under more oxidizing [$D(\text{Fe})_{\text{metal/silicate}} = 5.5$] conditions. For simplicity, partitioning values are calculated by partitioning of only iron and nickel [$D(\text{Ni})_{\text{metal/silicate}} = 26.5$] into the core.

are consistent with the accretion of a component of Earth's water and other volatile elements during the protoplanetary disk's lifetime. This may be achieved via the direct accretion of water adsorbed to dust (24, 25) or reflects the fact that the snowline will be inside of Earth's orbit toward the end of the protoplanetary disk's lifetime (5), allowing direct accretion of ice during this stage. Early accretion of a fraction of Earth's water budget is in excellent agreement with the detection of primordial water in Earth's deep mantle (26).

Our proposed timescale for the main phase of Earth's accretion and differentiation is shorter than typically inferred from ^{182}Hf - ^{182}W model ages of core formation (27). However, these ages are primarily controlled by the last reequilibration of the mantle during the Moon-forming impact event and are highly susceptible to model assumptions (28). Critically, the rapid timescales proposed here can be reconciled with Earth's mantle ^{182}W isotope composition if the Moon-forming impact occurred at least 40 Ma after the main accretion and differentiation of the proto-Earth (29). A late Moon-forming impact is supported by radiometric age dating of lunar anorthosites, which indicate that the crystallization of the lunar magma ocean occurred between 4.34 and 4.37 billion years ago (30).

MATERIALS AND METHODS

Iron isotope analyses

Whole rock samples weighing a few to hundreds of milligrams were digested using Savillex beakers with concentrated HF-HNO₃ mixtures

on a hotplate at 130°C. To ensure complete dissolution of enstatite and carbonaceous chondrite samples, they were further digested in Parr bombs at 210°C. Iron isotope composition of individual chondrules was determined using aliquots from which Zn (31) and Ca (18) have been previously separated. For the individual dissolution steps of Ivuna, iron was extracted from dissolution steps from which previously Sr (32), Cr (33), Mg (10), and Ca (10) have been separated and measured for their isotopic composition. The detailed dissolution procedure is fully described in (10).

Iron was separated from the matrix following published methods (34) using AG1-X4 anion exchange resin. Each iron separate typically consisted of several tens to hundreds of micrograms of iron, whereas procedural blanks are magnitudes lower, making blank correction inconsequential for our results. The Fe isotope compositions were measured using the Thermo Fisher Neptune Plus MC-ICP-MS (Multicollector–inductively coupled plasma mass spectrometry) at the Natural History Museum of Denmark in the medium-resolution mode. Samples were introduced to the plasma source using a stable introduction system (SIS, wet plasma) or an ESI Apex HR sample introduction system with an uptake of 25 $\mu\text{l min}^{-1}$ and analyzed at signal intensities of 0.30 to 0.45 nA on mass 56 for ~10-ppm iron solutions. Iron isotope data were acquired in static mode using four Faraday collectors setup as follows: ^{58}Fe and ^{57}Fe in the high-2 and high-1 collector on the high mass side of the axial Faraday, respectively; ^{56}Fe in the axial collector; and ^{54}Fe in the low-2 collector on the low mass side of the axial Faraday. Alongside the iron signal, the ^{60}Ni and ^{53}Cr beams were measured in the high-4 and low-4 collectors, respectively, to correct for direct isobar interferences on ^{54}Fe and ^{58}Fe from ^{54}Cr and ^{58}Ni , respectively. All Faraday cups collecting iron signals were connected to amplifiers with a 10^{11} -ohm feedback resistors, whereas the Faraday cups collecting the ^{60}Ni and ^{53}Cr signals were connected to amplifiers with 10^{12} -ohm feedback resistors. Measurements were made in the medium-resolution mode ($M/\Delta M > 5000$ as defined by the peak edge width from 5 to 95% full peak height) to resolve potential molecular interferences on the high-mass side (e.g., $^{40}\text{Ar}^{16}\text{O}^+$). We report our data relative to the IRMM-014 Fe isotope standard in the μ -notation, where the reported data represent the mean and SE of 10 individual standard-bracketed sample analyses, each comprising 25 \times 16.7 s of on-peak baseline measurement and 100 \times 16.7 s of sample measurement for all whole rock samples and stepwise dissolution steps where sufficient iron was available. The $\mu^{54}\text{Fe}$ notation refers to the deviation in the $^{54}\text{Fe}/^{56}\text{Fe}$ ratio when corrected for natural kinetic mass fractionation using a $^{57}\text{Fe}/^{56}\text{Fe}$ ratio of 0.023261 (35). In table S1, we also report the $^{57}\text{Fe}/^{56}\text{Fe}$ ratio normalized using a $^{54}\text{Fe}/^{56}\text{Fe}$ ratio of 0.062669 (35), which results in isotope variations and their uncertainties that are systematically halved but otherwise exhibiting the same relative variations, demonstrating that the choice of isotope ratio does not influence the interpretation of our results. Although the ^{58}Fe signal was monitored, we do not report the data, as the typical signal intensities during our analysis do not allow us to measure this isotope markedly above the noise level threshold of our 10^{11} -ohm feedback resistors. Moreover, the precision of the ^{58}Fe data is further compromised by a time variant interference correction from ^{58}Ni , which is introduced from the measured signal on ^{60}Ni . The ^{54}Cr signal contributing to the total ^{54}Fe signal was typically less than 1 ppm and, thus, negligible. On the basis of repeat analyses of processed iron separated from peridotite olivine (J12), DTS-2b and BHVO-2b standards ($n = 10$ including repeat analyses; 2 SD = 5.9 ppm) and intergroup isotopic

variability between ureilites ($n = 8$ including repeat analyses; 2 SD = 7.9 ppm), ordinary chondrites ($n = 9$; 2 SD = 7.7 ppm), and CI chondrites ($n = 9$ including repeat analyses; 2 SD = 8.2 ppm), we estimate the external reproducibility of a single $\mu^{54}\text{Fe}$ measurement to be better than ± 8.2 ppm (2 SD) (table S2).

Some mass-dependent fractionation of iron during planetary differentiation may occur by a nonkinetic process (i.e., equilibrium fractionation), and as such, our mass independent data for achondrites may include apparent nucleosynthetic variability arising from inappropriate mass fractionation correction, as we assume that mass-dependent fractionation occurred via kinetic processes. For example, Elardo and Shahar (36) suggested that iron isotope fractionation during core formation on terrestrial planets resulted in isotopically light mantles, which may have affected the mass bias–corrected iron isotope signatures determined for the mantles of Earth, Mars, Vesta, and the ureilite parent body determined here. Notably, Elardo and Shahar (36) argue that the terrestrial mantle is not fractionated relative to chondrites, and as such, their proposed mechanism cannot account for the CI-like iron isotope signature of Earth. We also note that average $\delta^{56}\text{Fe}$ compositions of noncarbonaceous achondrites reported here vary by only 0.07‰, which equates to a possible effect of less than 2 ppm, if the difference in mass-dependent isotope signature was solely due to equilibrium fractionation effects. This isotope effect is not resolvable given the current precision of our data and, critically, much smaller than the $\mu^{54}\text{Fe}$ variability of 14.6 ppm for the same samples. Hence, we conclude that nonkinetic mass fractionation cannot account for the vast majority of the observed $\mu^{54}\text{Fe}$ variability and is best understood as being primarily of nucleosynthetic in origin.

Calculation of hypothetical CI chondrite impactor mass

Growth via planetary collisions is the traditionally assumed mechanism of terrestrial planet growth. Only CI chondrites match the iron isotope signature of Earth's mantle. Thus, this isotope similarity may imply that most of the iron in the Earth's mantle today was delivered via a late impactor with CI chondrite composition after Earth's core had formed. To provide a conservative estimate of the mass of such a hypothetical impactor, we first determined the required minimum contribution of CI chondrite-like iron to Earth's mantle iron budget via a mixing calculation between CI ($\mu^{54}\text{Fe} = -2.0 \pm 2.7$ ppm) and EL chondrites ($\mu^{54}\text{Fe} = +6.4 \pm 0.7$ ppm). EL chondrites are, apart from CI chondrites, the meteorite group that is isotopically most similar to composition of Earth's mantle for $\mu^{54}\text{Fe}$ and, thus, serve as conservative proxy of the pre-impact mantle composition. Using these two end-members, we derived that approximately 70% of the iron in Earth's mantle today had to originate from the CI chondrite impactor. To estimate the relative mass of a hypothetical CI chondrite impactor based on the required iron contribution to the mantle, we assumed that 67% of the current mass of Earth is in the mantle and contains 6.26% iron (37). For the CI chondrite impactor, we used an iron abundance of 18.66% (9). Using these constraints, we calculated that the CI impactor was at least Mars sized but may have been substantially larger if the impactor metal did not fully equilibrate with the mantle.

Mixing calculations for continuous accretion

We calculated the isotopic evolution of an accreting Earth via addition of CI-like solids to an already formed planetesimal seed with iron and calcium isotope signatures akin to ureilites. For simplicity,

we assumed a constant iron concentration in the mantle and core during accretion. Accretion was simulated by adding material with a CI chondrite composition (9) to the growing Earth incrementally, and full isotopic equilibration between mantle and the accreted material was assumed in each step. Mixing calculations either consider a constant $D(\text{Fe})_{\text{metal/silicate}}$ of 5.5, 13.66, or 27.4 to simulate Earth's accretion under more oxidizing, similar or more reducing conditions than that of Earth today. We also partitioned nickel (Ni) into the core assuming a constant $D(\text{Ni})_{\text{metal/silicate}} = 26.5$. Given that calcium does not partition into the core, we used ^{48}Ca isotope data from (18) to calculate the evolving ^{48}Ca isotope signature of the accreting terrestrial mantle parallel to the ^{54}Fe signature. A terrestrial ^{48}Ca value ($= 0$) indicates that the mass the hypothetical Earth has accreted and, thus, at this point the calculated ^{54}Fe signature should also match that of the Earth's mantle today ($= 0$). Thus, this model provides a test for the approximate lower limit of $D(\text{Fe})_{\text{metal/silicate}}$ of Earth during its accretion via addition of CI-like solids. Without ongoing core formation before and during the accretion of the CI-like material, the iron and calcium isotope compositions would evolve along a linear mixing line between ureilites and CI chondrites and cannot generate an isotopic match in ^{54}Fe - ^{48}Ca space for Earth. Our approach allows us to constrain the major end-members that contributed to the growing Earth based on their isotopic signature, whereas their actual bulk chemical composition (e.g., C, N, and H_2O) may have been somewhat distinct from that preserved in the meteoritic record today. Hence, our model describes a general process rather than a precise chemical recipe.

SUPPLEMENTARY MATERIALS

Supplementary material for this article is available at <http://advances.sciencemag.org/cgi/content/full/6/7/eaay7604/DC1>

Supplementary Text

Table S1. Mass-independent $\mu^{54}\text{Fe}$ and $\mu^{57}\text{Fe}$ and mass-dependent $\delta^{56}\text{Fe}$ values for terrestrial and extraterrestrial materials relative to IRMM-14.

References (39–57)

REFERENCES AND NOTES

- A. Johansen, M. M. Low, P. Lacerda, M. Bizzarro, Growth of asteroids, planetary embryos, and Kuiper belt objects by chondrule accretion. *Sci. Adv.* **1**, e1500109 (2015).
- K. J. Walsh, A. Morbidelli, S. N. Raymond, D. P. O'Brien, A. M. Mandell, A low mass for Mars from Jupiter's early gas-driven migration. *Nature* **475**, 206–209 (2011).
- C. F. Chyba, The cometary contribution to the oceans of primitive Earth. *Nature* **330**, 632–635 (1987).
- A. Morbidelli, J. Chambers, J. I. Lunine, J. M. Petit, F. Robert, G. B. Valsecchi, K. E. Cyr, Source regions and timescales for the delivery of water to the Earth. *Meteorit. Planet. Sci.* **35**, 1309–1320 (2000).
- D. P. O'Brien, A. Izidoro, S. A. Jacobson, S. N. Raymond, D. C. Rubie, The delivery of water during terrestrial planet formation. *Space Sci. Rev.* **214**, 47 (2018).
- M. Fischer-Gödde, T. Kleine, Ruthenium isotopic evidence for an inner Solar System origin of the late veneer. *Nature* **541**, 525–527 (2017).
- K. Righter, M. J. Drake, Effect of water on metal-silicate partitioning of siderophile elements: A high pressure and temperature terrestrial magma ocean and core formation. *Earth Planet. Sci. Lett.* **171**, 383–399 (1999).
- V. Clesi, M. A. Bouhifd, N. Bolfan-Casanova, G. Manthilake, A. Fabbriozzi, D. Andrault, Effect of H_2O on metal-silicate partitioning of Ni, Co, V, Cr, Mn and Fe: Implications for the oxidation state of the Earth and Mars. *Geochim. Cosmochim. Acta* **192**, 97–121 (2016).
- H. Palme, K. Lodders, A. Jones, Solar system abundances of the elements, in *Treatise on Geochemistry* A. M. Davis, Ed., (Elsevier, ed. 2, 2014), vol. 2, pp. 15–36.
- M. Schiller, C. Paton, M. Bizzarro, Evidence for nucleosynthetic enrichment of the protosolar molecular cloud core by multiple supernova events. *Geochim. Cosmochim. Acta* **149**, 88–102 (2015).
- D. L. Cook, M. Schönbächler, Iron isotopic compositions of troilite (FeS) inclusions from iron meteorites. *Astron. J.* **154**, 172 (2017).
- J. E. Chambers, Planetary accretion in the inner Solar System. *Earth Planet. Sci. Lett.* **223**, 241–252 (2004).
- M. Schönbächler, R. W. Carlson, M. F. Horan, T. D. Mock, E. H. Hauri, Heterogeneous accretion and the moderately volatile element budget of Earth. *Science* **328**, 884–887 (2010).
- D. C. Rubie, D. J. Frost, U. Mann, Y. Asahara, F. Nimmo, K. Tsuchi, P. Kegler, A. Holzheid, H. Palme, Heterogeneous accretion, composition and core-mantle differentiation of the Earth. *Earth Planet. Sci. Lett.* **301**, 31–42 (2011).
- D. C. Rubie, S. A. Jacobson, A. Morbidelli, D. P. O'Brien, E. D. Young, J. de Vries, F. Nimmo, H. Palme, D. J. Frost, Accretion and differentiation of the terrestrial planets with implications for the compositions of early-formed Solar System bodies and accretion of water. *Icarus* **248**, 89–108 (2015).
- E. M. van Kooten, D. Wielandt, M. Schiller, K. Nagashima, A. Thomen, K. K. Larsen, M. B. Olsen, Å. Nordlund, A. N. Krot, M. Bizzarro, Isotopic evidence for primordial molecular cloud material in metal-rich carbonaceous chondrites. *Proc. Natl. Acad. Sci. U.S.A.* **113**, 2011–2016 (2016).
- J. Zhang, N. Dauphas, A. M. Davis, I. Leya, A. Fedkin, The proto-Earth as a significant source of lunar material. *Nat. Geosci.* **5**, 251–255 (2012).
- M. Schiller, M. Bizzarro, V. A. Fernandes, Isotopic evolution of the protoplanetary disk and the building blocks of Earth and the Moon. *Nature* **555**, 507–510 (2018).
- N. Hosono, S. I. Karato, J. Makino, T. R. Saitoh, Terrestrial magma ocean origin of the Moon. *Nat. Geosci.* **12**, 418–423 (2019).
- J. Bollard, J. N. Connelly, M. Bizzarro, Pb-Pb dating of individual chondrules from the CBachondrite Gubja: Assessment of the impact plume formation model. *Meteorit. Planet. Sci.* **50**, 1197–1216 (2015).
- J. Siebert, J. Badro, D. Antonangeli, F. J. Ryerson, Terrestrial accretion under oxidizing conditions. *Science* **339**, 1194–1197 (2013).
- J. Badro, A. S. Côté, J. P. Brodholt, A seismologically consistent compositional model of Earth's core. *Proc. Natl. Acad. Sci. U.S.A.* **111**, 7542–7545 (2014).
- J. Badro, J. P. Brodholt, H. Piet, J. Siebert, F. J. Ryerson, Core formation and core composition from coupled geochemical and geophysical constraints. *Proc. Natl. Acad. Sci. U.S.A.* **112**, 12310–12314 (2015).
- M. J. Drake, Origin of water in the terrestrial planets. *Meteorit. Planet. Sci.* **40**, 519–527 (2005).
- L. Vattuone, M. Smerieri, L. Savio, A. M. Asaduzzaman, K. Muralidharan, M. J. Drake, M. Rocca, Accretion disc origin of the Earth's water. *Philos. Trans. R. Soc. A* **371**, 20110585 (2013).
- L. J. Hallis, G. R. Huss, K. Nagashima, G. J. Taylor, S. A. Halldórsson, D. R. Hilton, M. J. Mottl, K. J. Meech, Evidence for primordial water in Earth's deep mantle. *Science* **350**, 795–797 (2015).
- T. Kleine, M. Touboul, B. Bourdon, F. Nimmo, K. Mezger, H. Palme, S. B. Jacobsen, Q. Z. Yin, A. N. Halliday, Hf-W chronology of the accretion and early evolution of asteroids and terrestrial planets. *Geochim. Cosmochim. Acta* **73**, 5150–5188 (2009).
- R. A. Fischer, F. Nimmo, Effects of core formation on the Hf-W isotopic composition of the Earth and dating of the Moon-forming impact. *Earth Planet. Sci. Lett.* **499**, 257–265 (2018).
- G. Yu, S. B. Jacobsen, Fast accretion of the Earth with a late Moon-forming giant impact. *Proc. Natl. Acad. Sci. U.S.A.* **108**, 17604–17609 (2011).
- L. E. Borg, A. M. Gaffney, C. K. Shearer, A review of lunar chronology revealing a preponderance of 4.34–4.37 Ga ages. *Meteorit. Planet. Sci.* **50**, 715–732 (2015).
- J. Bollard, J. N. Connelly, M. J. Whitehouse, E. A. Pringle, L. Bonal, J. K. Jørgensen, Å. Nordlund, F. Moynier, M. Bizzarro, Early formation of planetary building blocks inferred from Pb isotopic ages of chondrules. *Sci. Adv.* **3**, e1700407 (2017).
- C. Paton, M. Schiller, M. Bizzarro, Identification of an ^{84}Sr -depleted carrier in primitive meteorites and implications for thermal processing in the solar protoplanetary disk. *Astrophys. J. Lett.* **763**, L40 (2013).
- M. Schiller, E. van Kooten, J. C. Holst, M. B. Olsen, M. Bizzarro, Precise measurement of chromium isotopes by MC-ICPMS. *J. Anal. At. Spectrom.* **29**, 1406–1416 (2014).
- N. Dauphas, P. E. Janney, R. A. Mendybaev, M. Wadhwa, F. M. Richter, A. M. Davis, M. van Zuilen, R. Hines, C. N. Foley, Chromatographic separation and multicollection-ICPMS analysis of iron. Investigating mass-dependent and -independent isotope effects. *Anal. Chem.* **76**, 5855–5863 (2004).
- J. Völkering, D. A. Papanastassiou, Iron isotope anomalies. *Astrophys. J.* **347**, L43–L46 (1989).
- S. M. Elardo, A. Shahar, Non-chondritic iron isotope ratios in planetary mantles as a result of core formation. *Nat. Geosci.* **10**, 317–321 (2017).
- W. F. McDonough, S. S. Sun, The composition of the Earth. *Chem. Geol.* **120**, 223–253 (1995).
- N. Dauphas, H. H. Chen, J. Zhang, D. A. Papanastassiou, A. M. Davis, C. Travaglio, Calcium-48 isotopic anomalies in bulk chondrites and achondrites: Evidence for a uniform isotopic reservoir in the inner protoplanetary disk. *Earth Planet. Sci. Lett.* **407**, 96–108 (2014).
- A. Trinquier, T. Elliott, D. Ulfbeck, C. Coath, A. N. Krot, M. Bizzarro, Origin of nucleosynthetic isotope heterogeneity in the solar protoplanetary disk. *Science* **324**, 374–376 (2009).
- C. Burkhardt, T. Kleine, F. Oberli, A. Pack, B. Bourdon, R. Wieler, Molybdenum isotope anomalies in meteorites: Constraints on solar nebula evolution and origin of the Earth. *Earth Planet. Sci. Lett.* **312**, 390–400 (2011).
- H. Tang, N. Dauphas, Abundance, distribution, and origin of ^{60}Fe in the solar protoplanetary disk. *Earth Planet. Sci. Lett.* **359**, 248–263 (2012).

42. H. Tang, N. Dauphas, ^{60}Fe - ^{60}Ni chronology of core formation in Mars. *Earth Planet. Sci. Lett.* **390**, 264–274 (2014).
43. J. Zhang, N. Dauphas, A. M. Davis, A. Pourmand, A new method for MC-ICPMS measurement of titanium isotopic composition: Identification of correlated isotope anomalies in meteorites. *J. Anal. At. Spectrom.* **26**, 2197–2205 (2011).
44. A. Trinquier, J.-L. Birck, C. L. Allegre, Widespread ^{54}Cr heterogeneity in the inner solar system. *Astrophys. J.* **655**, 1179–1185 (2007).
45. A. Yamakawa, K. Yamashita, A. Makishima, E. Nakamura, Chromium isotope systematics of achondrites: Chronology and isotopic heterogeneity of the inner solar system bodies. *Astrophys. J.* **720**, 150–154 (2010).
46. L. Qin, C. M. O'D. Alexander, R. W. Carlson, M. F. Horan, T. Yokoyama, Contributors to chromium isotope variation of meteorites. *Geochim. Cosmochim. Acta* **74**, 1122–1145 (2010).
47. R. W. Carlson, M. Boyet, M. Horan, Chondrite barium, neodymium, and samarium isotopic heterogeneity and early earth differentiation. *Science* **316**, 1175–1178 (2007).
48. M. Boyet, ^{142}Nd evidence for early (>4.53 Ga) global differentiation of the silicate Earth. *Science* **309**, 576–581 (2005).
49. L. E. Borg, G. A. Brennecka, S. J. Symes, Accretion timescale and impact history of Mars deduced from the isotopic systematics of martian meteorites. *Geochim. Cosmochim. Acta* **175**, 150–167 (2016).
50. F. Moynier, J. M. D. Day, W. Okui, T. Yokoyama, A. Bouvier, R. J. Walker, F. A. Podosek, Planetary-scale strontium isotopic heterogeneity and the age of volatile depletion of early Solar System materials. *Astrophys. J.* **758**, 45 (2012).
51. U. Hans, T. Kleine, B. Bourdon, Rb–Sr chronology of volatile depletion in differentiated protoplanets: BABI, ADOR and ALL revisited. *Earth Planet. Sci. Lett.* **374**, 204–214 (2013).
52. N. R. Clayton, Oxygen isotopes in meteorites. *Annu. Rev. Earth Planet. Sci.* **21**, 115–149 (1993).
53. M. Fischer-Gödde, C. Burkhardt, T. S. Kruijer, T. Kleine, Ru isotope heterogeneity in the solar protoplanetary disk. *Geochim. Cosmochim. Acta* **168**, 151–171 (2015).
54. W. Akram, M. Schönbächler, S. Bisterzo, R. Gallino, Zirconium isotope evidence for the heterogeneous distribution of s-process materials in the solar system. *Geochim. Cosmochim. Acta* **165**, 484–500 (2015).
55. K. R. Bermingham, E. A. Worsham, R. J. Walker, New insights into Mo and Ru isotope variation in the nebula and terrestrial planet accretionary genetics. *Earth Planet. Sci. Lett.* **487**, 221–229 (2018).
56. S. Goderis, A. D. Brandon, B. Mayer, M. Humayun, S-Process Os isotope enrichment in ureilites by planetary processing. *Earth Planet. Sci. Lett.* **431**, 110–118 (2015).
57. J. M. D. Day, R. J. Walker, L. Qin, D. Rumble III, Late accretion as a natural consequence of planetary growth. *Nat. Geosci.* **5**, 614–617 (2012).

Acknowledgments

Funding: Financial support for this project was provided by the Danish National Research Foundation (DNRF97) and the European Research Council (ERC Consolidator Grant Agreement 616027—STARDUST2ASTEROIDS) to M.B. **Author contributions:** M.S. designed and performed the research. M.S. and M.B. analyzed the data and wrote the manuscript with input from J.S. **Competing interests:** The authors declare that they have no competing interests. **Data and materials availability:** All data needed to evaluate the conclusions in the paper are present in the paper and/or the Supplementary Materials. Additional data related to this paper may be requested from the authors.

Submitted 16 July 2019

Accepted 26 November 2019

Published 12 February 2020

10.1126/sciadv.aay7604

Citation: M. Schiller, M. Bizzarro, J. Siebert, Iron isotope evidence for very rapid accretion and differentiation of the proto-Earth. *Sci. Adv.* **6**, eaay7604 (2020).

Iron isotope evidence for very rapid accretion and differentiation of the proto-Earth

Martin Schiller, Martin Bizzarro and Julien Siebert

Sci Adv **6** (7), eaay7604.

DOI: 10.1126/sciadv.aay7604

ARTICLE TOOLS

<http://advances.sciencemag.org/content/6/7/eaay7604>

SUPPLEMENTARY MATERIALS

<http://advances.sciencemag.org/content/suppl/2020/02/10/6.7.eaay7604.DC1>

REFERENCES

This article cites 56 articles, 12 of which you can access for free
<http://advances.sciencemag.org/content/6/7/eaay7604#BIBL>

PERMISSIONS

<http://www.sciencemag.org/help/reprints-and-permissions>

Use of this article is subject to the [Terms of Service](#)

Science Advances (ISSN 2375-2548) is published by the American Association for the Advancement of Science, 1200 New York Avenue NW, Washington, DC 20005. The title *Science Advances* is a registered trademark of AAAS.

Copyright © 2020 The Authors, some rights reserved; exclusive licensee American Association for the Advancement of Science. No claim to original U.S. Government Works. Distributed under a Creative Commons Attribution NonCommercial License 4.0 (CC BY-NC).